JOURNAL OF MATERIALS SCIENCE **40** (2005) 1979– 1985

Piezoelectric and magnetic properties of PZT-$(Ni_{0.284}Zn_{0.549}Cu_{0.183})Fe_{1.984}O_4$ composites

HSIEN-KUANG LIU*, JIN. H. HUANG
Department of Mechanical and Computer Aided Engineering, Feng-Chia University, 100 Wenhwa Road, 407 Taichung, Taiwan, Republic of China
E-mail: hkliu@fcu.edu.tw

CHIH-WEN HSIEH, HSIN-TSUNG TU
Eleceram Technology Co., Ltd., No. 231, LungShou St., Taoyuan, Taiwan, Republic of China

The piezoelectric/piezomagnetic composite, PZT/$Ni_{0.284}Zn_{0.549}Cu_{0.183}Fe_{1.984}O_4$, was fabricated by the mixed oxide method. The phase assemblage, piezoelectric strain constant and saturation magnetization were investigated. The results indicate that the PZT phase is compatible with $Ni_{0.284}Zn_{0.549}Cu_{0.183}Fe_{1.984}O_4$ phase, and dense diphasic ceramic composites were obtained. It is found that piezoelectric strain constant decreases exponentially as the amount of doped piezomagnetic materials in the composite increases. Correspondingly, saturation magnetization of the composite also decreases with the increasing weight fraction of piezoelectric materials. Three reasons cause the results. First, the grain growth of piezomagnetic phase at the co-sintering temperature reduces grain size and continuity of the piezoelectric phase. Second, the pore size and porosity in composite increase dramatically with increasing amount of piezomagnetic phase. Third, the low resistivity of the composite prevents the poling process and reduces the piezoelectric strain constant. The tailoring of microstructure to achieve a high performance piezoelectric/piezomagnetic composite is proposed based on the analysis.

1. Introduction

Recently, the studies of piezoelectric/piezomagnetic (PE/PM) composites have attracted a great amount of attention. Theoretically it was proposed that the magnetoelectric (ME) coupling effect in the composite of PE fiber reinforced PM matrix [1–5] could amplify electric field 10 to 100 times higher than a single piezoelectric or piezomagnetic material such as Cr_2O_3, $TbFeO_3$. However, it was seldom experimentally verified. Some experimental attempts to realize strong ME effect in PZT/$BaTiO_3$ composites were unsuccessful due to possible causes including microcracks, defects, impurities, and incompatible structural and thermal properties of the two phases [6, 7]. Boomgaard [6] synthesized PE/PM composites composed of $BaTiO_3$ and $CoFe_2O_4$ by sintering and unidirectional solidification of eutectic melts. The composites developed microcracks due to thermal expansion mismatch and yielded ME coefficients that were one order smaller than calculated values [8]. Up to now, most researchers in this field concentrate on the theoretical aspects, including C. W. Nan [8], Harshe [9] Avellaneda [10] and Benveniste [5]. According to Nan, the magnetoelectric effect results from the elastic interaction between two phases. The mechanism is that when a magnetic field is applied to a composite, the ferrite particles change their shape because of magnetostriction, and the strain is passed along to the piezoelectric particles, resulting in an electrical polarization. In spite of good magnetoelectric coupling effect in composites proposed by theoretical studies, the experimental value is three order smaller than the theoretical one. The possible reasons include presence of extra phase, difficult in poling, and a complex connectivity pattern of the component phases. In Harshe and Avellaneda's pioneering work [9, 10], a multilayer structure is expected to be superior as a ME composite because a large dielectric constant can be obtained by shortening the thickness of piezomagnetic layers. However, mismatch of thermal and mechanical properties between PE and PM layers may be a challenge during fabrication. Based on the idea, Srinivasan [11] found a compatible material, lanthanum manganites (LMO), to combine with PZT by a multilayer method. In addition, LMO showed a giant magnetostriction and metallic conduction.

The PE/PM composites are of high interest for a variety of device applications including magnetoelectric memory devices, electrically controlled microwave phase shifters or ferromagnetic resonance devices, magnetically controlled electro-optic or piezoelectric

* Author to whom all correspondence should be addressed.

devices, broad band magnetic field sensors [12], smart sensors, and actuators. To enhance the promising applications, it is necessary to better understand the PE/PM composites, a new class of intelligent materials, with tailored properties.

In this paper, a piezoelectric/piezomagnetic composite with peculiar compositions is fabricated and their properties are evaluated. There are two basic approaches for the fabrication of the composite: mixed oxide method and multilayer method. It is more difficult to fabricate the composite by the multilayer method due to thermal stresses caused by thermal expansion mismatch. Therefore, this paper concentrates on the fabrication of PZT/$Ni_{0.284}Zn_{0.549}$-$Cu_{0.183}Fe_{1.984}O_4$ composites by mixed oxide method. The research topics cover (1) the effect of relative weight fraction of the constituents on properties of composites, and (2) the correlation between the microstructure and PE and PM properties.

2. Experimental

Piezoelectric/piezomagnetic composites consisting of lead zirconate titanate and Ni-Zn-Cu ferrite are processed with nine different weight fractions, as shown in Table I. The preparation of both constituents and their composites is depicted as follows.

2.1. Materials

The piezomagnetic material to be processed is $Ni_{0.284}Zn_{0.549}Cu_{0.183}Fe_{1.984}O_4$. It is fabricated by the mixed oxide method using the following four kinds of constituent powders: NiO, ZnO, CuO, and Fe_2O_3. The purity of the four constituents is all 99.9%. The average powder size for the four constituents is respectively 1, 1.5, 10 and 0.05 μm. The weight of each constituent is measured to match the requirement of mole fraction in the piezomagnetic material. Then those powders are well mixed with deionized water and zirconia balls in a ball milling machine, calcinated at 900°C for 2 hours, and finally grinded in a ball milling machine in order to reduce particle size. After the above three steps, the piezomagnetic powders with spinel-structure phases are obtained and ready to combine with PZT powders.

The piezoelectric material used is the high performance lead zirconate titanate (PZT, $PbZrO_3$-$PbTiO_3$, 52/48 wt%) powders with average particle size of 1 μm. The powder is provided by Eleceram Technology Co., Ltd., Taiwan. The PZT powder is then doped into the piezomagnetic powders according to designed weight fraction. After the doping process, mixing, calcination, and grinding processes are followed in order to obtain uniformly distributed raw powders.

2.2. Processing

The flow chart of processing of piezoelectric-piezomagnetic composites is shown in Fig. 1. The well mixed PZT and piezomagnetic powders are then coated by PVA (polyvinyl alcohol) solution by a granulation process. The amount of PVA addition is around 12.5–17 wt% that of total amount of powders. The particle size after granulation is controlled in the range of 150–250 μm. The mixture of powders and PVA is then put into a cylindrical powder pressing mold, and pressed uniaxially under pressure of 120 MPa to obtain a disk green composite with diameter 15 mm and thickness 1.36 mm. Then the binder in green composite is burned out in a high temperature oven at 550°C for 4 h. Finally the green composite is sintered at 1100°C for 6 h to yield the piezoelectric/ piezomagnetic composite.

2.3. Characterization

Before measuring physical properties of the piezoelectric/piezomagnetic composite, the poling process is conducted in silicon oil under a highly intense electric field of 35 KV/cm and temperature of 80°C, followed by a magnetization process. The piezoelectric strain constant is measured by d_{33} meter (Berlincourt Piezo d-Meter, U.S.A.) under 100 Hz. In order to correlate the properties and the microstructure, XRD analysis and SEM observation are conducted. Saturation magnetization is measured by vibration sample magnetometer (VSM, EG&G Model-PAR 4500) after poling process.

3. Results and discussion

3.1. Piezoelectric properties

Fig. 2a shows the X-ray diffraction (XRD) pattern of pure PZT ceramics, while Fig. 2b shows the XRD pattern of pure $Ni_{0.284}Zn_{0.549}Cu_{0.183}Fe_{1.984}O_4$ ceramics (ferrite). Both figures are depicted as the reference

TABLE I Physical properties as a function of composition of the PZT/ferrite composite

Composition	[PZT:Ferrite] (wt%)	Porosity (%)	Average pore size (μm)	Density (g/cm^3)	Resistivity (Ω-cm)	Piezoelectric strain constant (pC/N)	Saturation magnetization (emu/g)
A	[100:0]	6.68	0	7.93	2.03×10^{11}	751	1.98
B	[90:10]	7.35	9	6.91	6.99×10^{9}	251	2.73
C	[80:20]	8.02	13	6.50	9.23×10^{8}	38	5.97
D	[60:40]	8.03	17	6.05	4.85×10^{8}	25	6.92
E	[40:60]	8.04	20	5.81	4.17×10^{8}	20	6.96
F	[20:80]	8.46	–	5.42	3.55×10^{8}	18	7.04
G	[10:90]	9.51	–	5.21	2.93×10^{8}	15	7.28
H	[5:95]	10.04	–	5.18	1.17×10^{8}	12	9.75
I	[0:100]	10.57	–	5.13	1.13×10^{8}	10	62

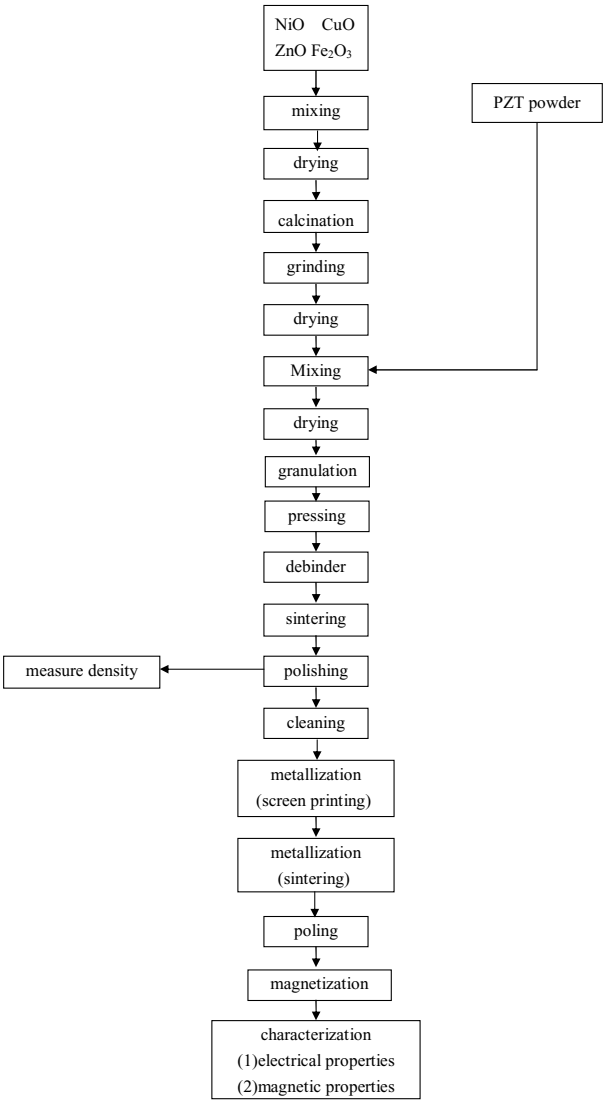

Figure 1 Flow chart of the fabrication of piezoelectric/piezomagnetic composites.

for patterns of piezoelectric/piezomagnetic (PE/PM) composites with compositions of 90/10 wt%, 80/20 wt%, 60/40 wt%, and 40/60 wt% as shown in following Fig. 2c–f, respectively. Compared the four figures to Fig. 2a, the highest peak value of XRD intensity corresponding to pervoskite phase of PZT all occurs at 2θ equal to 31.5°; however, the peak height gradually decreases due to the increasing addition of ferrite in the composite. In Figs. 2c through 2f, the highest peak value of XRD intensity corresponding to spinel phase of ferrite occurs at 2θ equal to 35.5°, and the peak value gradually increases due to the increasing addition of ferrite. For XRD patterns of composites shown in Fig. 2c through 2f, peaks for pervoskite and spinel phases match well with corresponding PZT pattern (Fig. 2a) and ferrite pattern (Fig. 2b), suggesting that there is no third phase existed in composites. However, the decreasing extent of XRD intensity of PZT in composite caused by the addition of ferrite is not proportional to its composition. The following equation allows analyzing this phenomenon

$$\text{PZT\%} = \frac{I_{\text{PZT}}}{I_{100\ \text{wt\%\ PZT}}} \tag{1}$$

I_{PZT} represents diffraction intensity of piezoelectric phase in the composite, while $I_{100\ \text{wt\%\ PZT}}$ stands for that in 100 wt% PZT. For the 60/40 wt% PZT/ferrite composite, the diffraction intensity of corresponding piezoelectric phase (12285 CPS) is 54.86% that of pure PZT (22395 CPS). The inequality of XRD intensity (54.86%) and composition (60%) of PZT suggests that interaction occur between perovskite and spinel structures.

Fig. 3 depicts the piezoelectric strain constant d_{33} of composite as a function of weight percentage of PZT. It can be observed that d_{33} increases with weight percentage of PZT in composite via a sharp exponential function. This figure also demonstrates that the addition of Ni-Zn-Cu ferrite powders in the PZT powders during the fabrication of the composite dramatically reduces the piezoelectric effect. Several aspects lead to the result. First, the hard inclusions of Ni^{+2}, Zn^{+2}, and Cu^{+2} existed in Ni-Zn-Cu ferrite phase for the composite serve as acceptors in the PZT matrix because their electric charge is lower than those ionics such as Ti^{+4} and Zr^{+4} in the PZT. Therefore, the hard inclusions generate a large amount of oxygen vacancies in the piezoelectric phase, and this results in the difficulty of movement and rotation of walls between various electric domains as well as the reduction of the poling effect. Therefore, d_{33} reduces significantly.

3.2. Piezomagnetic properties

Counterpart effect can be found for the relation between saturation magnetization (M_s) and weight percentage of PZT in the PE/PM composite. As shown in Fig. 4, the saturation magnetization decreases significantly with increasing weight percentage of PZT by an inversely exponential function. As the perovskite structure of the PZT can not be magnetized, the addition of the PZT in the $Ni_{0.284}Zn_{0.549}Cu_{0.183}Fe_{1.984}O_4$ matrix reduces the effect of magnetization, yielding the lower saturation magnetization.

Our results are compared to those in Yu *et al.* [13]. For $x = 0.1$, 0.2, 0.4 and 0.7 in the $(1 - x)$ $BaTiO_3$-$x(Ni_{0.3}Zn_{0.7})Fe_{2.1}O_4$ for Yu's system, the saturation magnetization (M_s) is respectively 0.09, 5.16, 21.61, and 31.42 emu/g. While for $x = 0.1$, 0.2, 0.4 and 0.6 in our system $(1 - x)$PZT-$x$$Ni_{0.284}Zn_{0.549}Cu_{0.183}Fe_{1.984}$-$O_4$, the saturation magnetization is respectively 2.73, 5.97, 6.92, and 6.96 emu/g. It is found that lower content of ferrite ($x = 0.1$) in our system seems to have higher saturation magnetization; however, the increase of saturation magnetization with content of ferrite tends to be steady in the medium content of ferrite (x value), but lower than those in Yu's system. It has to be noted that the saturation magnetization for pure $Ni_{0.284}Zn_{0.549}Cu_{0.183}Fe_{1.984}O_4$ and $(Ni_{0.3}Zn_{0.7})Fe_{2.1}O_4$ is respectively 62 and 100 emu g^{-1}. The key composition seems to be Cu. According to Shrotri *et al.* [14], the increase of Cu composition decreases saturation magnetization in the Ni-Zn-Cu ferrite. The decrease in M_s may be attributed to the substitution of Ni by Cu having a lower magnetic moment.

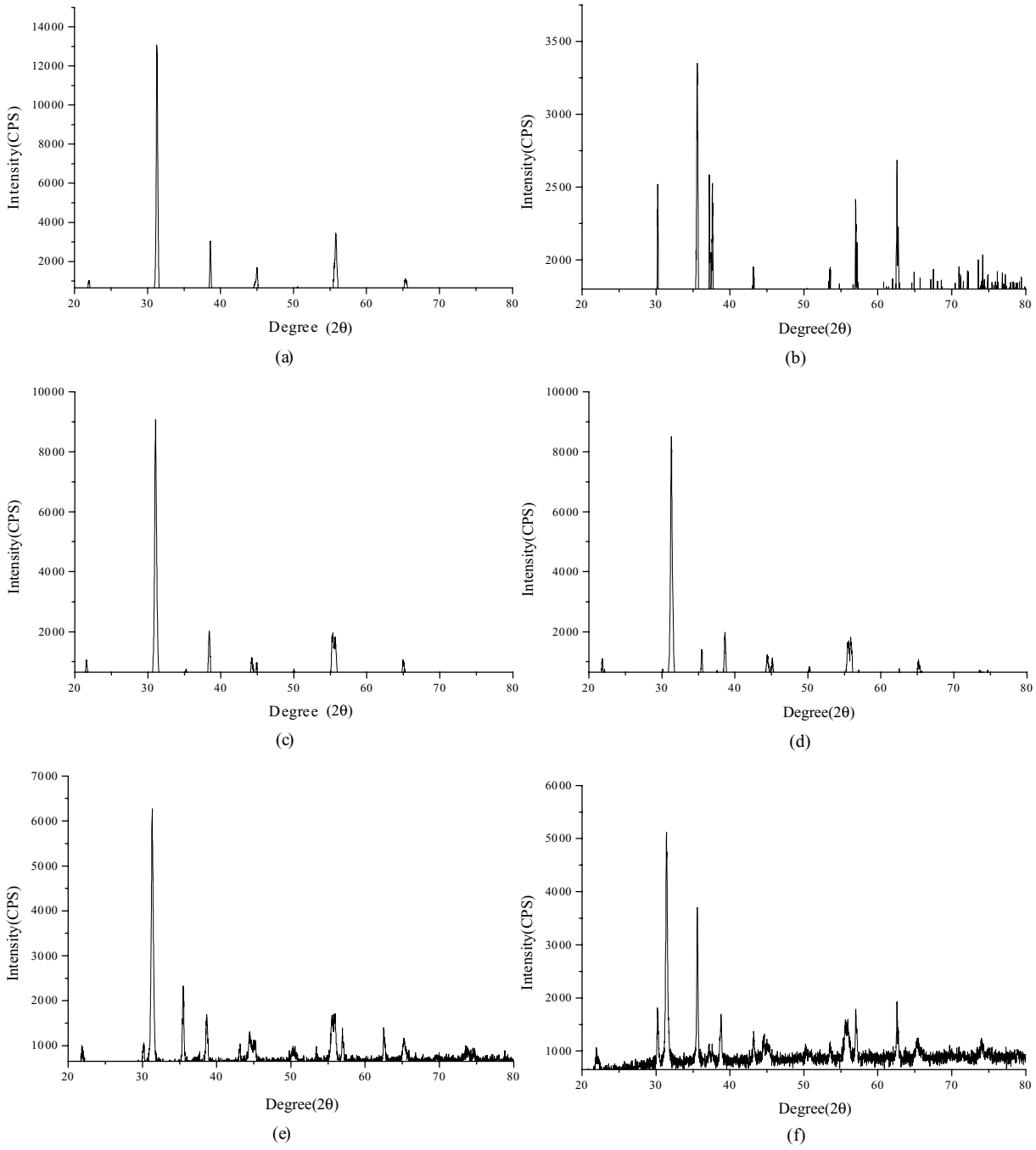

Figure 2 X-ray diffraction patterns of (a) PZT, (b) $Ni_{0.284}Zn_{0.549}Cu_{0.183}Fe_{1.984}O_4$ ferrite, (c) 90 wt% PZT/10 wt% ferrite, (d) 80 wt% PZT/20 wt% ferrite, (e) 60 wt% PZT/40 wt% ferrite, (f) 40 wt% PZT/60 wt% ferrite.

3.3. Evolution of microstructure

In order to obtain a super magnetoelectric (ME) effect in the composite, three criteria have to be satisfied [15]: first, no chemical reaction occurs between compositions; second, the resistivity of the piezomagnetic phase should be as high as possible; third, mechanical defects such as pores at the interface between the two phases should not exist. It has already been verified in XRD results of Section 3.1 that no third phase other than PZT and ferrite has been found indicating there is no chemical reaction.

Due to existence of Pb in PZT, its resistivity ρ of $2.03 \times 10^{11}\Omega$-cm is higher than the allowable value of 10^{10} Ω-cm for poling process. In contrast, good electrical conductivity of the composition of Fe_2O_3 in Ni-Zn-Cu ferrite leads to its lower ρ of 10^8 Ω-cm, which is markedly lower than suitable value of $10^{10}\Omega$-cm for poling. This would make poling process difficult because part of electric current in the poling electric field passed through the ferrite easily instead of conducting poling on the PZT. Therefore, electric domain wall of PZT cannot move easily, and leading to short-range ordering of electric dipoles. An attempt was adopted by raising poling electric field to overcome the above problem; nevertheless, the higher electric field damaged the specimen because it was higher than the collapsed voltage. Results for resistivity of composites are shown in Table I. It can be found that only

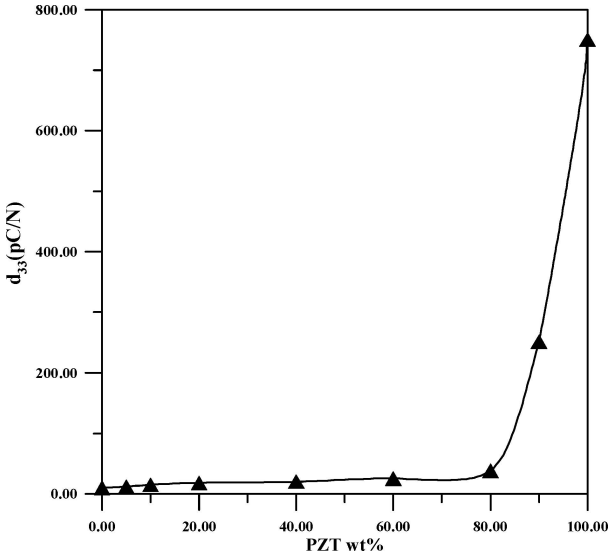

Figure 3 The piezoelectric strain constant of composite as a function of weight percentage of PZT.

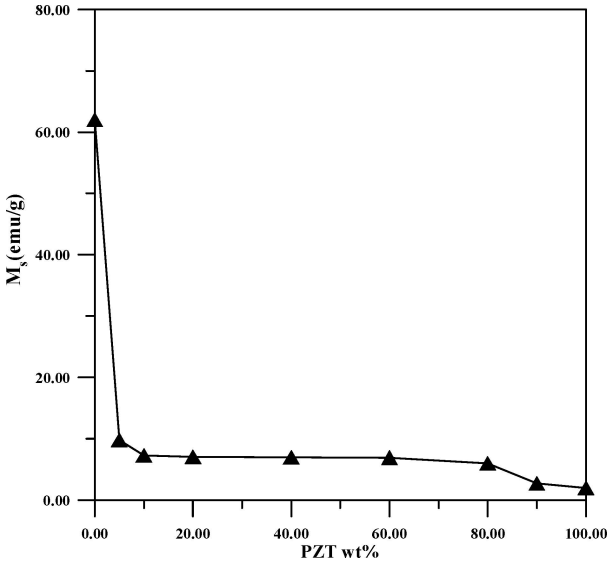

Figure 4 Saturation magnetization of composite as a function of weight percentage of PZT.

compositions A and B have resistivity higher than or close to the allowable value of 10^{10} Ω-cm for poling process. This also correlates well with piezoelectric strain constant d_{33} in Fig. 3 that compositions A (100 wt% PZT) and B (90 wt% PZT) have higher d_{33} values.

For 60/40 wt% PZT/ferrite composite, the XRD intensity of piezoelectric phase is 54.86% that of pure PZT; however, d_{33} of the composite (24.75pC/N) is only 3.3% that of pure PZT(751pC/N). The answer for the very difference can be drawn from the SEM observation. Fine and uniform grains with grain size around 2–6 μm are observed in the Fig. 5a for the microstructure of pure PZT; furthermore, almost no pores can be observed. On the other hand, in Fig. 5b the microstructure of Ni-Zn-Cu ferrite shows larger grain size around 70 μm and few pores at the grain boundary. However, when the two compositions are co-sintered at 1100°C, more and larger pores evolve, which are not observed in pure PZT or ferrite. For example, as shown in Fig. 5c, a 90/10 wt% piezoelectric/piezomagnetic composite depicts extensive pores with size around 8–10 μm, and grain size between those for PZT and ferrite. This figure suggests that PZT grains be coalesced and still connected. When the amount of ferrite increases to 20 wt%, the pore size gradually increases to 13 μm as shown in Fig. 5d. Furthermore, the addition of 20 wt% ferrite in the composite not only increases the pore size, but also raises porosity of the composite from 7.35 to 8.02% as shown in Table I; and the porosity seems to increase with the raising amount of ferrite in composite. The large pore size indicates uneven shrinkage at the grain boundary between PZT and ferrite, and this leads to lower piezoelectric and piezomagnetic performance. It is found that the porosity remains almost the same for compositions C (PE/PM: 80/20 wt%), D (60/40 wt%), and E (40/60 wt%) in Table I; however, the pore size keeps increasing up to 17 μm (composition D) and 20 μm (composition E), as shown in Fig. 5e respectively. A trend is inferred from Fig. 5c to f by three stages: first, dispersion of ferrite in connected PZT; second, grain growth of ferrite reduces grain size of PZT and inter-separates each other; third, ferrite grains connect.

The pore size growth is probably due to mismatch strain in the grain boundary between ferrite/PZT caused by differential thermal expansion. Thermal expansion coefficient α for PZT and Ni-Zn-Cu ferrite is respectively 1.8×10^{-6}/°C and 9.0×10^{-6}/°C. The composite was cooled to shrink after it was sintered to 1100°C. However, larger shrinkage (higher α) of the ferrite is constrained by smaller shrinkage (lower α) of surrounded PZT, leading to pores at the interface. As the ratio of the ferrite in the composite increases, the amount of shrinkage increases but the constraint from PZT decreases, resulting in increasing pore size.

The adopted sintering temperature of 1100°C may be appropriate for that of PZT; however, it is higher than sintering temperature of 1050°C for Ni-Zn-Cu ferrite. This leads to extra growth of ferrite grain and pores. Table I also shows that density decreases as the addition of ferrite in composite increases. This corresponds to increasing pore size when more ferrite is added in the composite. For higher ferrite ratio in the composite, connectivity of ferrite phase due to extra growth of ferrite grain makes it difficult to get high ME effects [15]. A higher sintering temperature in the range of 1100–1250°C is suggested to enlarge the grain size of PZT and break the connectivity of ferrite.

Although, composites shown in this work do not perform better piezoelectric or piezomagnetic effects when the piezomagnetic or piezoelectric compositions are added, the mixed oxide method shows the easier process than the multiplayer method. By controlling parameters such as sintering temperature, pressure, and distribution of constitutents, the mixed oxide method may be used to fabricate a composite consisting of not only product effect, but multi-port effect—an effect that allows applying magnetic or electric field in any location in the composite.

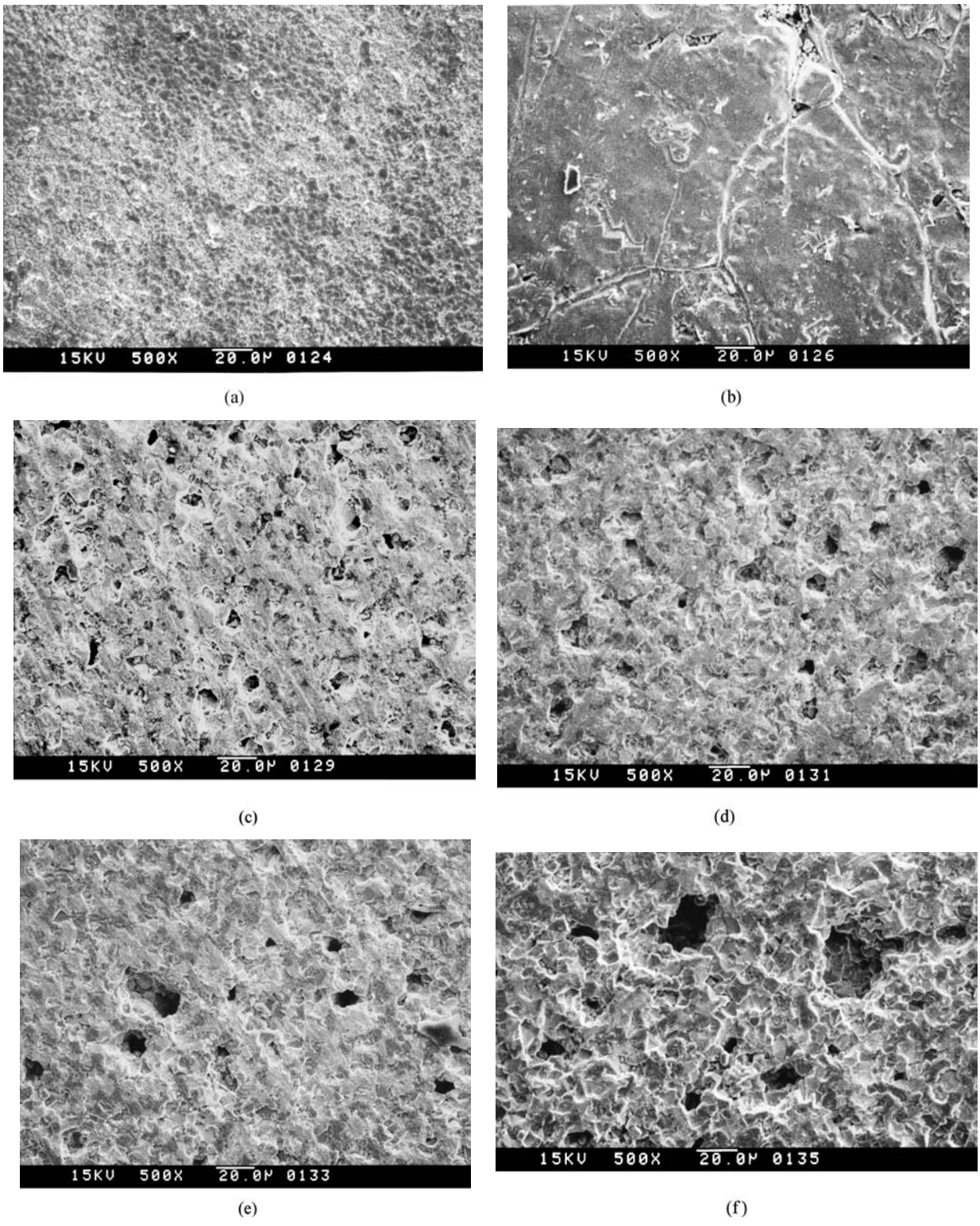

Figure 5 SEM micrographs of (a) PZT ceramics with fine and uniform microstructure, (b) $Ni_{0.284}Zn_{0.549}Cu_{0.183}Fe_{1.984}O_4$ ferrite with larger grain size and few pores, (c) 90/10 wt% piezoelectric/piezomagnetic (PZT/ferrite) composite with medium grain size and extensive pores with pore size of 8 to 10 μm, (d) 80/20 wt% PZT/ferrite composite with increasing pore size of 13 μm, (e) 60/40 wt% PZT/ferrite composite with pore size of 17 μm, (f) larger pore size of 20 μm in 40/60 wt% PZT/ferrite composite.

4. Conclusions

This study shows that diphasic ceramic composites consisting of piezoelectric PZT and piezomagnetic $Ni_{0.284}Zn_{0.549}Cu_{0.183}Fe_{1.984}O_4$ can be successfully fabricated. The two phases are verified by XRD without extra third phase. This indicates that the PZT phase is compatible with $Ni_{0.284}Zn_{0.549}Cu_{0.183}Fe_{1.984}O_4$ phase. Poling effect of PZT ceramics in the composite is dramatically reduced due to the addition of Ni, Zn, Cu ionics. This may be solved by fabrication of the composite using lamination method; however, the mismatch of thermal expansion between two compositions needs to be tailored during the sintering stage. Reduced piezoelectric strain constant and saturation magnetization in the composite compared to those of corresponding pure piezoelectric and piezomagnetic materials are caused

by the discontinuity in the piezoelectric phase. Grain growth of the ferrite reduces the grain size of the piezoelectric phase and enlarges the pores. Both contribute to the discontinuity and may be improved by suitably controlling sintering temperature or using hot-pressing. Another effective method is to fabricate PZT fibers by sol-gel method, and this would provide the continuity of the piezoelectric phase.

Acknowledgments

Authors would be grateful for the financial support from National Science Council in Taiwan under the contract No. NSC 91-2745-P-035-004 and NSC 92-2216-E-035-007, and professor Tsung-Shune Chin in Department of Materials Science and Engineering, National Tsing-Hua University for providing vibration sample magnetometer (VSM, EG&G Model-PAR 4500).

References

1. J. H. HUANG and W. S. KUO, *J. Appl. Phys.* **81**(3) (1997) 4889.
2. J. H. HUANG, *ibid.* **78** (1995) 6491.
3. J. H. HUANG and W. S. KUO, *Acta Metallurgica et Materialia* **44**(12) (1997) 4889.
4. J. H. HUANG, Y. H. CHIU and H. K. LIU, *J. Appl. Phys.* **83**(10) (1998) 5364.
5. Y. BENVENISTE, *Phys. Rev.* B. **16**(51) (1994) 424.
6. J. V. D. BOOMGAARD, D. R. TERREL and R. A. J. BORN, *J. Mat. Sci.* **9** (1974) 1705.
7. J. V. D. BOOMGAARD, A. M. J. G. VAN RUN and J. VAN SUCHTELEN, *Ferroelectrics* **14** (1976) 727.
8. C. W. NAN, *Phys. Rev.* B **50** (1994) 6082.
9. G. HARSHE, J. P. DOUGHERTY and R. E. NEWNHAM, *Int. J. Appl. Electromagn. Mater* **4** (1993) 145.
10. M. AVELLANEDA and G. HARSHE, *J. Intell. Mater. Syst. Struct.* **5** (1994) 501.
11. G. SRINIVASAN, National Science Foundation Proposal No. 0072144, U.S.A. (1999).
12. L. P. M. BRACKE and R. G. VAN VLIET, *Int. J. Electronics* **51**(3) (1981) 255.
13. Z. YU and C. ANG, *J. Mat. Sci.* **13** (2002) 193.
14. J. J. SHROTRI, S. D. KULKARNI, C. E. DESHPANDE, A. MITRA, S. R. SAINKAR, P. S. ANIL KUMAR and S. K. DATE, *Mater. Chem. Phys.* **59** (2002) 1.
15. J. RYU, S. PRIYA, K. UCHINO and H-E. KIM, *J. Electroceram.* **8** (2002) 107.

Received 26 August
and accepted 24 November 2004